Conservative Numerical Schemes for the Vlasov Equation.

Francis Filbet,
IECN-INRIA projet Numath - Université de Nancy I
BP 239, 54506 Vandœuvre-lès-Nancy cedex, France.

Eric Sonnendrücker,
IRMA - Université Louis Pasteur,
7 rue R. Descartes, 67084 Strasbourg, France.

Pierre Bertrand,
LPMI - Université de Nancy I
BP 239, 54506 Vandœuvre-lès-Nancy cedex, France.

Abstract

A new scheme for solving the Vlasov equation using a phase space grid is proposed. The algorithm is based on the conservation of the flux of particles, and the distribution function is reconstructed using different techniques allowing to control spurious oscillations or preserving the positivity. Several numerical results are presented in two and four dimensional phase space and the scheme is compared with the semi-lagrangian method. This method is almost as accurate as the semi-lagrangian one, and the local reconstruction technique is well suited to do parallel computation.

The Vlasov equation describes the evolution of a system of particles under the effects of self-consistent electro magnetic fields. The unknown $f(t,x,v)$, depending on the time t, the position x, and the velocity v, represents the distribution function of particles (electrons, ions,...) in phase space. This model can be used for the study of beam propagation or of a collisionless plasma.

The numerical resolution of the Vlasov equation is usually performed by particle methods (PIC) which consist in approximating the plasma by a finite number of macro-particles. The trajectories of these particles are computed from the characteristic curves given by the Vlasov equation, whereas self-consistent fields are computed on a mesh of the physical space. This method allows to obtain satisfying results with a few number of particles (we refer to Birdsall-Langdon for more details [1]). However, it is well known that the numerical noise inherent to the particle method becomes too important to have a precise description of the distribution function in phase space. Moreover, the numerical noise only decreases in $1/\sqrt{N}$ when the number of particles N is increased. To remedy to this problem, methods discretizing the Vlasov equation on a mesh of phase space have been proposed. Among them, the Fourier-Fourier transform is based on a Fast Fourier Transform of the distribution function in phase space, but this method is only valid for periodic boundary conditions [8, 9]. Consequently, for non periodic boundary conditions, Gibbs oscillations form at the boundary of the grid and become source of spurious oscillations which propagate into the distribution

function. A finite element method has also been proposed [16, 17]. This method is well suited to handling complicated boundaries which may arise in many practical applications, but it requires the numerical resolution of a system which is an inconvenient to deal with the Vlasov equation in high dimension. The semi-lagrangian method, which consists in computing the distribution function at each grid point by following the characteristic curves backward, is also used. To compute the origin of the characteristic a high order interpolation method is needed. E. Sonnendrücker *et al.* proposed the cubic spline reconstruction which gives very good results [13, 14], but the use of spline interpolation destroys the local character of the reconstruction. Nakamura and Yabe also presented the Cubic Interpolated Propagation (CIP) method based on the approximation of the gradients of the distribution function in order to use a Hermite interpolation [15]. This method is very expensive in memory computation since it needs the storage of f, $\nabla_x f$, and $\nabla_v f$. Another scheme for the Vlasov equation is the Flux Corrected Transport (FCT) [3, 4] or more recently the Flux Balance Method (FBM) [6]: the basic idea of this method is to compute the average of the Vlasov equation solution in each cell of the phase space grid by a conservative method .

One of the common flaws of these algorithms is the non preservation of the positivity which is an inconvenient for long time simulation since numerical oscillations develop. The goal of this paper is to propose a new scheme, the Positive and Flux Conservative (PFC) method, giving a good approximation of the distribution function, the conservation of mass, and the preservation of positivity. Moreover, the use of a local interpolation allows to do straightforward and scalable parallel computation.

This paper is organized as follows: In the first part, we briefly describe the Vlasov equation, recalling some properties of the solution, like the conservation of the entropy, L^p norms, and the energy. Then, we present the conservative method for the discretization of a transport equation, using the characteristic curves, and we give different reconstruction techniques which enable us to control spurious oscillations. In the last section, we present numerical results in the two and four dimensional phase space to compare the different schemes with the semi-lagrangian method.

1 The Vlasov equation

The evolution of the density of particles $f(t,x,v)dx\,dv$ in the phase space $(x,v) \in \mathbb{R}^d \times \mathbb{R}^d$, $d = 1,..,3$, is given by the Vlasov equation,

$$\frac{\partial f}{\partial t} + v \cdot \nabla_x f + F(t,x,v) \cdot \nabla_v f = 0, \tag{1}$$

where the force field $F(t,x,v)$ is coupled with the distribution function f giving a non linear system. We mention the well known Vlasov-Poisson (VP) and Vlasov-Maxwell (VM) models describing the evolution of particles under the effects of self-consistent electro magnetic fields: we first define the charge density $\rho(t,x)$ and current density $j(t,x)$ by

$$\rho(t,x) = q \int_{\mathbb{R}^d} f(t,x,v)dv, \quad j(t,x) = q \int_{\mathbb{R}^d} v\, f(t,x,v)\, dv, \tag{2}$$

where q is the single charge. The force field is given for the Vlasov-Poisson model by

$$F(t,x,v) = \frac{q}{m} E(t,x), \quad E(t,x) = -\nabla_x \phi(t,x), \quad -\Delta_x \phi = \frac{\rho}{\varepsilon_0}, \tag{3}$$

where m represents the mass of one particle. For the Vlasov-Maxwell system, we have

$$F(t,x,v) = \frac{q}{m} \left(E(t,x) + v \wedge B(t,x)\right), \tag{4}$$

and E, B are solution of the Maxwell equations

$$\begin{cases} \dfrac{\partial E}{\partial t} - c^2 \mathrm{curl} B = -\dfrac{j}{\varepsilon_0}, \\ \dfrac{\partial B}{\partial t} + \mathrm{curl} E = 0, \\ \mathrm{div} E = \dfrac{\rho}{\varepsilon_0}, \quad \mathrm{div} B = 0, \end{cases} \tag{5}$$

with the compatibility condition

$$\frac{\partial \rho}{\partial t} + \mathrm{div} j = 0, \tag{6}$$

which is verified by the Vlasov equation solution.

We now recall some classical a priori estimates on the (VP) and (VM) systems: first of all assuming the initial data $f_0(x,v)$ is positive, the solution $f(t,x,v)$ remains positive for all t. Next, observing that $\mathrm{div}_{x,v}\left(v, F(t,x,v)\right) = 0$, we immediately deduce that for all function $\beta \in C^1(\mathbb{R}^+, \mathbb{R}^+)$,

$$\frac{d}{dt} \int_{\mathbb{R}^d \times \mathbb{R}^d} \beta(f(t,x,v)) dx dv = 0, \quad \forall t \in \mathbb{R}^+.$$

In particular all L^p norms, for $1 \leq p \leq +\infty$, are preserved. Moreover, taking $\beta(r) = r \ln(r)$, we obtain the conservation of the kinetic entropy

$$\frac{d}{dt} H(t) = \frac{d}{dt} \int_{\mathbb{R}^d \times \mathbb{R}^d} f(t,x,v) \, \ln\left(f(t,x,v)\right) dx dv = 0, \quad \forall t \in \mathbb{R}^+.$$

Next multiplying the Vlasov equation by $|v|^2$, and integrating by parts, we find the conservation of energy for the (VP) system

$$\frac{d}{dt} \int_{\mathbb{R}^d \times \mathbb{R}^d} f(t,x,v) \, |v|^2 dx dv + \int_{\mathbb{R}^d} |E(t,x)|^2 dx = 0, \quad \forall t \in \mathbb{R}^+,$$

and for the (VM) system

$$\frac{d}{dt} \int_{\mathbb{R}^d \times \mathbb{R}^d} f(t,x,v) \, |v|^2 dx dv + \int_{\mathbb{R}^d} |E(t,x)|^2 + |B(t,x)|^2 dx = 0, \quad \forall t \in \mathbb{R}^+.$$

Finally, note the Vlasov equation also preserves mass and impulsion,

$$\frac{d}{dt} \int_{\mathbb{R}^d \times \mathbb{R}^d} f(t,x,v) \begin{pmatrix} 1 \\ v \end{pmatrix} dx dv = 0, \quad \forall t \in \mathbb{R}^+.$$

2 The conservative method

In this section, we will introduce conservative discretizations of the Vlasov equation and propose several reconstruction techniques. Unlike classical eulerian algorithms as finite difference or finite volume schemes, this method is not restricted by a CFL condition on the time step. The Vlasov equation coupled with the Poisson equation or the Maxwell system often contains filamentation, which is one of the major issues one has to deal with when constructing a numerical scheme. Indeed, the distribution function $f(t,x,v)$ is constant along the characteristic curves which become close so that phase space regions where $f(t,x,v)$ has different values come close together and steep gradients are generated. At some time in the simulation, the phase space grid becomes too coarse to follow these thin filaments. The different gridded methods briefly presented in the introduction do not have any mechanism to distinguish numerical oscillations and filamentation. The algorithm should effectively be high order in regions of the problem where the concept of order is related usefully to accuracy, and should control oscillations where gradients are large or where the distribution function goes to zero. The conservative method presented below is derived from these requirements.

The starting point of our method is the Flux Balance method [6], discretizing the Vlasov equation in the conservative form : we first observe that by a standard time splitting scheme, we can restrict ourselves, without loss of generality, to a one dimensional problem which leads to solve the following problem,

$$\partial_t f + \partial_x \left(\mathrm{u}(t,x)\, f\right) = 0, \quad \forall (t,x) \in \mathbb{R}^+ \times [x_{min}, x_{max}]. \tag{7}$$

We will assume that $\mathrm{u}(t,x)$ is smooth enough for example u is Lipschitz continuous. Then we can define the characteristic curves solution of the differential system corresponding to the transport equation:

$$\begin{cases} \dfrac{dX}{ds}(s) = \mathrm{u}(s, X(s)), \\ X(t) = x. \end{cases} \tag{8}$$

Let us note $X(s,t,x)$ the solution of (8) and define the Jacobian $J(s,t,x) = \partial_x X(s,t,x)$. In [2], it is proved that $J(s,t,x)$ is positive for all $(s,t,x) \in \mathbb{R}^+ \times \mathbb{R}^+ \times \mathbb{R}$, and the solution of the transport equation (7) can be expressed as

$$f(t,x) = f(s, X(s,t,x))\, J(s,t,x), \tag{9}$$

which describes the conservation of particles along the characteristic curves

$$\forall K \subset \mathbb{R}, \quad \int_K f(t,x)dx = \int_{X(s,t,K)} f(s,x)dx, \tag{10}$$

where

$$X(s,t,K) = \{y \in \mathbb{R} : \quad y = X(s,t,z); \quad z \in K\}.$$

This property remains true if $d \geq 1$. Now, let us introduce a finite set of mesh points $(x_{i+1/2})_{i \in I}$ of the computational domain (x_{min}, x_{max}), we will denote by $\Delta x = x_{i+1/2} - x_{i-1/2}$, and $C_i =$

$[x_{i-1/2}, x_{i+1/2}]$. Assume the values of the distribution function are known at time $t^n = n\,\Delta t$, we find the new values at time t^{n+1} by integration of the distribution function on each sub-interval. Thus using the conservation of particles (10) and recalling that the Jacobian function $x \mapsto J(t^n, t^{n+1}, x)$ is positive, we have

$$\int_{x_{i-1/2}}^{x_{i+1/2}} f(t^{n+1}, x)dx = \int_{X(t^n,t^{n+1},x_{i-1/2})}^{X(t^n,t^{n+1},x_{i+1/2})} f(t^n, x)dx,$$

then, we set

$$\Phi_{i+1/2}(t^n) = \int_{X(t^n,t^{n+1},x_{i+1/2})}^{x_{i+1/2}} f(t^n, x)dx,$$

to finally obtain the conservative scheme

$$\int_{x_{i-1/2}}^{x_{i+1/2}} f(t^{n+1}, x)dx = \Phi_{i-1/2}(t^n) \; + \int_{x_{i-1/2}}^{x_{i+1/2}} f(t^n, x)dx \; - \; \Phi_{i+1/2}(t^n). \tag{11}$$

The evaluation of the average of the solution over $[x_{i-1/2}, x_{i+1/2}]$ allows to ignore small details of the exact solution which may be very costly to compute.

In the general situation, we cannot explicitly compute the characteristic curves, we need to introduce a time discretization of (8). Using a second order leap-frog scheme, we obtain a fixed point problem, where we look for $x^n = X(t^n, t^{n+1}, x_{i+1/2})$ such that

$$\begin{cases} x_{i+1/2} - x^n = \Delta t\, u(t^{n+1/2}, x^{n+1/2}), \\ t^{n+1/2} = t^n + \dfrac{\Delta t}{2}, \quad x^{n+1/2} = \dfrac{x_{i+1/2} + x^n}{2}, \end{cases}$$

which can be iteratively solved. Note that most of the time in kinetic transport equations, the time splitting scheme allows to avoid this situation since the characteristic curves become straight lines.

The main step is now to choose an efficient method to reconstruct the distribution function from the values in each cell C_i. In [6], E. Fijalkow only used a linear interpolation, but this method does not give a positive scheme and does not control spurious oscillations. The method proposed by Boris and Book [3] or the use of classical slope limiters is too dissipative to give an accurate description of the distribution function. Here, we shall use a reconstruction via primitive function: let $F(t^n, .)$ be a primitive of the distribution function $f(t^n, .)$, we denote by

$$f_i^n = \frac{1}{\Delta x} \int_{x_{i-1/2}}^{x_{i+1/2}} f(t^n, x)dx,$$

then we have $F(t^n, x_{i+1/2}) - F(t^n, x_{i-1/2}) = \Delta x f_i^n$, and

$$F(t^n, x_{i+1/2}) = \Delta x \sum_{k=0}^{i} f_k^n = w_i^n.$$

In the sequel, the time variable t^n only acts as a parameter and will be dropped. We present two different methods of reconstruction.

2.1 The ENO reconstruction

The ENO (Essentially Non Oscillatory) method has been introduced by Harten *et al.* in [7]. It is often used for the discretization of hyperbolic equations and allows to control spurious oscillations. Unlike classical conservation laws, the Vlasov equation solution does not develop any shock, but stiff gradients appear in the phase space. Thus, the ENO reconstruction seems to be useful to treat this problem. We first recall the divided difference formula which plays an important role in this method

$$\begin{aligned} F[x_{i+1/2}, x_{i+3/2}, .., x_{i+p+1/2}] = & \quad \frac{F[x_{i+3/2}, .., x_{i+p+1/2}] - F[x_{i+1/2}, .., x_{i+p-1/2}]}{x_{i+p+1/2} - x_{i+1/2}}, \\ F[x_{i+1/2}] = F(x_{i+1/2}) = & \; w_i, \end{aligned} \tag{12}$$

and satisfies the property

- If $F(x) \in C^p([x_{i+1/2}, x_{i+p+1/2}])$, then

$$\exists \zeta \in (x_{i+1/2}, x_{i+p+1/2}), \quad F[x_{i+1/2}, x_{i+3/2}, .., x_{i+p+1/2}] = \frac{1}{p!} \frac{d^p F}{dx^p}(\zeta).$$

- If the k-th derivative of $F(x)$ is discontinuous with $0 \leq k \leq p$ on the interval $[x_{i+1/2}, x_{i+p+1/2}]$, then

$$F[x_{i+1/2}, x_{i+3/2}, .., x_{i+p+1/2}] = O(\Delta x^{k-p})\, [\omega^{(k)}],$$

where $[\omega^{(k)}]$ represents the jump of the k-th derivative. The ENO reconstruction consists in choosing the stencil for which the approximation is the smoothest, i.e. the divided difference is the smallest in module: on the interval $[x_{i-1/2}, x_{i+1/2}]$, we first define $q_1(x)$, the polynomial of degree one, interpolating the function $F(x)$ at $x_{i-1/2}$ and $x_{i+1/2}$,

$$q_1(x) = w_{i-1} + (x - x_{i-1/2}) \frac{w_i - w_{i-1}}{\Delta x},$$

and we set $d_1(i) = i$. Let us assume that we have constructed the polynomial of degree k interpolating the function $F(x)$ at the points

$$x_{d_k(i)-1/2}, ..., x_{d_k(i)+k-1/2}.$$

To find the polynomial $q_{k+1}(x)$, we consider $k+2$ points obtained by adding to the previous ones the first point on the left or on the right, and choose the point for which the divided difference is the smallest:

$$d_{k+1}(i) = \begin{cases} d_k(i) - 1 & \text{if } |F[x_{d_k(i)-3/2}, .., x_{d_k(i)+k-1/2}]| \leq |F[x_{d_k(i)-1/2}, .., x_{d_k(i)+k+1/2}]|, \\ d_k(i) & \text{else.} \end{cases}$$

We continue the algorithm until the order we want.

Proposition 2.1 *Let us assume the function F(x) is r+1 continuously differentiable and define its piecewise polynomial approximation denoted by $F_h(x)$ such that*

$$\forall x \in [x_{i-1/2}, x_{i+1/2}], \quad F_h(x) = q_r(x),$$

where $q_r(x)$ is the polynomial of degree r constructed by following the previous method, then

- $\dfrac{d^k q_r}{dx^k}(x) = \dfrac{d^k F}{dx^k}(x) + O(\Delta x^{r+1-k}), \quad 0 \leq k \leq r,$
- $q_r(x_{j+1/2}) = F(x_{j+1/2}), \quad \forall j \in \{d_{r(i)-1/2}, ..., d_{r(i)+r-1/2}\},$
- $q_r(x)$ *is an essentially non-oscillatory reconstruction in the sense that*

$$TV[q_r(.)] \leq TV[F(.)] + O(\Delta x^{r+1}),$$

where the total variation of a function $F(.)$ is the number given by the following limit

$$TV[F(.)] = \limsup_{\varepsilon \to 0} \frac{1}{\varepsilon} \int |F(x+\varepsilon) - F(x)| dx.$$

The last inequality implies that spurious oscillations are controlled at the order $r+1$ (see [7]). From this high order accurate reconstruction, we can define the quantity $\Phi_{i+1/2}(t^n)$ by

$$\Phi_{i+1/2}(t^n) = \int_{X(t^n, t^{n+1}, x_{i+1/2})}^{x_{i+1/2}} f(t^n, x) dx = F_h(x_{i+1/2}) - F_h(X(t^n, t^{n+1}, x_{i+1/2})).$$

This method has been implemented up to the fourth order. It is not positive but allows to control spurious oscillations.

2.2 The Positive and Flux Conservative method

As previously, we use the reconstruction via primitive function but the stencil is now fixed. To ensure the preservation of positivity and the maximum principle, we introduce a slope corrector. Indeed, it is only by sacrificing the high order requirement when the gradients are very steep, that we can hope to obtain a positive algorithm. In the sequel, we denote by $f_\infty = \max_{j \in I} \{f_j\}$.

The second order approximation: let us assume for simplicity the propagating velocity $u(t,x)$ is positive, then we build a first approximation on the interval $[x_{i-1/2}, x_{i+1/2}]$ using the points $\{x_{i-1/2}, x_{i+1/2}, x_{i+3/2}\}$:

$$\tilde{F}_h(x) = w_{i-1} + (x - x_{i-1/2}) f_i + \frac{1}{2}(x - x_{i-1/2})(x - x_{i+1/2}) \frac{f_{i+1} - f_i}{\Delta x},$$

where we use that $w_i - w_{i-1} = \Delta x \, f_i$. Thus by differentiation, we obtain a second order accurate approximation of the distribution function on the interval $[x_{i-1/2}, x_{i+1/2}]$:

$$\tilde{f}_h(x) = \frac{d\,\tilde{F}_h}{dx}(x) = f_i + (x - x_i) \frac{f_{i+1} - f_i}{\Delta x}.$$

But, this approximation does not satisfy the maximum principle and spurious oscillations may occur, then we introduce a slope corrector:

$$\epsilon_i = \begin{cases} \min\Big(1; 2\, f_i/(f_{i+1} - f_i)\Big) & \text{if } f_{i+1} - f_i > 0, \\ \min\Big(1; -2\,(f_\infty - f_i)/(f_{i+1} - f_i)\Big) & \text{if } f_{i+1} - f_i < 0, \end{cases} \tag{13}$$

and finally obtain the following approximation:

$$f_h(x) = f_i + \epsilon_i (x - x_i) \frac{f_{i+1} - f_i}{\Delta x}, \quad \forall x \in [x_{i-1/2}, x_{i+1/2}]. \tag{14}$$

From this construction, the following proposition is obvious:

Proposition 2.2 *The approximation defined by (14) satisfies:*

- *The conservation of the average: for all* $i \in I$, $\int_{x_{i-1/2}}^{x_{i+1/2}} f_h(x)dx = \Delta x\, f_i$.
- *The maximum principle: for all* $x \in (x_{min}, x_{max})$, $0 \le f_h(x) \le f_\infty$.

Moreover, if we assume the Total Variation of the distribution function $f(x)$ *is bounded, then we obtain the global estimate:*

$$\int_{x_{min}}^{x_{max}} |f_h(x) - \tilde{f}_h(x)|dx \le \Delta x \sum_i (1 - \epsilon_i)|f_{i+1} - f_i| \le TV(f)\, \Delta x.$$

Now, we can define an approximation of the flux $\Phi_{i+1/2}(t^n)$: we first find the cell C_j such that $X(t^n, t^{n+1}, x_{i+1/2}) \in C_j$ and set $\alpha_i = x_{j+1/2} - X(t^n, t^{n+1}, x_{i+1/2})$, which satisfies $0 \le \alpha_i \le \Delta x$, then

$$\Phi_{i+1/2}(t^n) = \int_{x_{j+1/2}-\alpha_i}^{x_{i+1/2}} f(t^n, x)dx = \alpha_i \left[f_j + \frac{\epsilon_j}{2}\left(1 - \frac{\alpha_i}{\Delta x}\right)(f_{j+1} - f_j)\right] + \Delta x \sum_{k=j+1}^{i} f_k.$$

By symmetry, we find an approximation of $\Phi_{i+1/2}(t^n)$ when the propagating velocity $\mathrm{u}(t, x)$ is negative, we set $\alpha_i = x_{j-1/2} - X(t^n, t^{n+1}, x_{i+1/2})$, then $-\Delta x \le \alpha_i \le 0$ and

$$\Phi_{i+1/2}(t^n) = \int_{x_{j-1/2}-\alpha_i}^{x_{i+1/2}} f(t^n, x)dx = \alpha_i \left[f_j - \frac{\epsilon_j}{2}\left(1 + \frac{\alpha_i}{\Delta x}\right)(f_j - f_{j-1})\right] + \Delta x \sum_{k=i+1}^{j-1} f_k,$$

where ϵ_j is given by

$$\epsilon_j = \begin{cases} \min\Big(1; 2\,(f_\infty - f_j)/(f_j - f_{j-1})\Big) & \text{if } f_j - f_{j-1} > 0, \\ \min\Big(1; -2\, f_j/(f_j - f_{j-1})\Big) & \text{if } f_j - f_{j-1} < 0, \end{cases} \tag{15}$$

Third order approximation: we now extend the previous method for the third order reconstruction. On the interval $[x_{i-1/2}, x_{i+1/2}]$, we use the stencil $\{x_{i-3/2}, x_{i-1/2}, x_{i+1/2}, x_{i+3/2}\}$ to approximate the primitive and as previously we introduce a slope corrector to finally obtain for all $x \in C_i$,

$$\begin{aligned} f_h(x) &= f_i + \frac{\epsilon_i^+}{6\,\Delta x^2}\Big[2\,(x-x_i)(x-x_{i-3/2}) + (x-x_{i-1/2})(x-x_{i+1/2})\Big](f_{i+1}-f_i) \\ &- \frac{\epsilon_i^-}{6\,\Delta x^2}\Big[2\,(x-x_i)(x-x_{i+3/2}) + (x-x_{i-1/2})(x-x_{i+1/2})\Big](f_i-f_{i-1}), \end{aligned} \tag{16}$$

with

$$\epsilon_i^+ = \begin{cases} \min\Big(1; 2\,f_i/(f_{i+1}-f_i)\Big) & \text{if } f_{i+1}-f_i > 0, \\ \min\Big(1; -2\,(f_\infty - f_i)/(f_{i+1}-f_i)\Big) & \text{if } f_{i+1}-f_i < 0, \end{cases} \tag{17}$$

and

$$\epsilon_i^- = \begin{cases} \min\Big(1; 2\,(f_\infty - f_i)/(f_i-f_{i-1})\Big) & \text{if } f_i-f_{i-1} > 0, \\ \min\Big(1; -2\,f_i/(f_i-f_{i-1})\Big) & \text{if } f_i-f_{i-1} < 0. \end{cases} \tag{18}$$

Proposition 2.3 *The approximation of the distribution function $f_h(x)$ defined by (16)-(18) constructed using the third order method satisfies*

- *The conservation of the average: for all $i \in I$, $\int_{x_{i-1/2}}^{x_{i+1/2}} f_h(x)dx = \Delta x\, f_i$.*
- *The maximum principle: for all $x \in (x_{min}, x_{max})$, $0 \le f_h(x) \le f_\infty$.*

Moreover, if we assume the Total Variation of the distribution function $f(x)$ is bounded, then we obtain the global estimate:

$$\int_{x_{min}}^{x_{max}} |f_h(x) - \tilde{f}_h(x)|\,dx \le 4\,TV(f)\,\Delta x,$$

where $\tilde{f}_h$ denotes the third order approximation of f without slope corrector.

Proof. Let us consider $x \in C_i = [x_{i-1/2}, x_{i+1/2}]$ and denote by

$$\begin{aligned} \alpha(x) &= \frac{1}{\Delta x^2}\Big[2\,(x-x_i)(x-x_{i-3/2}) + (x-x_{i-1/2})(x-x_{i+1/2})\Big], \\ \beta(x) &= \frac{1}{\Delta x^2}\Big[2\,(x-x_i)(x-x_{i+3/2}) + (x-x_{i-1/2})(x-x_{i+1/2})\Big]. \end{aligned}$$

It is easy to check that

$$\int_{x_{i-1/2}}^{x_{i+1/2}} \alpha(x)dx = \int_{x_{i-1/2}}^{x_{i+1/2}} \beta(x)dx = 0,$$

then the conservation of the average immediately follows. To obtain the preservation of positivity, assuming the values $(f_j)_j$ are positive, we observe that in the cell C_i, the function $\alpha(x)$ is increasing whereas $\beta(x)$ decreases and $\alpha(x)$, $\beta(x) \in [-1, 2]$. Then, we split $f_h(x)$ as the sum of $h(x)$ and $g(x)$ with

$$h(x) = \frac{1}{3}\left[f_i + \frac{\alpha(x)}{2}\epsilon_i^+(f_{i+1} - f_i)\right], \quad \text{and} \quad g(x) = \frac{1}{3}\left[2\,f_i - \frac{\beta(x)}{2}\epsilon_i^-(f_i - f_{i-1})\right].$$

The function $h(x)$ (*resp.* $g(x)$) is only a combination of f_i and f_{i+1} (*resp.* f_{i-1} and f_i), then from the value of ϵ_i^+ (*resp.* ϵ_i^-), it is easy to prove that $h(x)$ (*resp.* $g(x)$) is positive. Using a similar decomposition, we also prove that $f_h(x)$ is bounded by f_∞.
Now, we prove the global estimate on the positive reconstruction:

$$\begin{aligned}
\int_{x_{min}}^{x_{max}} |f_h(x) - \tilde{f}_h(x)|dx &= \sum_i \int_{x_{i-1/2}}^{x_{i+1/2}} |\ \alpha(x)\,(1-\epsilon_i^+)[f_{i+1} - f_i] + \beta(x)\,(1-\epsilon_i^-)[f_i - f_{i-1}]\ |\ dx \\
&\leq 2\,\Delta x \sum_i (1-\epsilon_i^+)|f_{i+1} - f_i| + 2\,\Delta x \sum_i (1-\epsilon_i^-)|f_i - f_{i-1}| \\
&\leq 4\,\Delta x \sum_i |f_{i+1} - f_i| \leq 4\,\Delta x\, TV(f). \qquad \square
\end{aligned}$$

From this reconstruction, we approximate the quantity $\Phi_{i+1/2}(t^n)$, by looking for the cell C_j such that $X(t^n, t^{n+1}, x_{i+1/2}) \in C_j$ and setting $\alpha_i = x_{j+1/2} - X(t^n, t^{n+1}, x_{i+1/2})$. Then for a positive propagating velocity, we obtain

$$\begin{aligned}
\Phi_{i+1/2}(t^n) &= \int_{x_{j+1/2}-\alpha_i}^{x_{i+1/2}} f(t^n, x)dx = \Delta x \sum_{k=j+1}^{i} f_k\ + \\
&+ \alpha_i \left[f_j + \frac{\epsilon_j^+}{6}\left(1 - \frac{\alpha_i}{\Delta x}\right)\left(2 - \frac{\alpha_i}{\Delta x}\right)(f_{j+1} - f_j) + \frac{\epsilon_j^-}{6}\left(1 - \frac{\alpha_i}{\Delta x}\right)\left(1 + \frac{\alpha_i}{\Delta x}\right)(f_j - f_{j-1})\right],
\end{aligned}$$

and when $\mathrm{u}(t, x)$ is negative, we set $\alpha_i = x_{j-1/2} - X(t^n, t^{n+1}, x_{i+1/2})$, then $-\Delta x \leq \alpha_i \leq 0$ and

$$\begin{aligned}
\Phi_{i+1/2}(t^n) &= \int_{x_{j-1/2}-\alpha_i}^{x_{i+1/2}} f(t^n, x)dx = \Delta x \sum_{k=i+1}^{j-1} f_k\ + \\
&+ \alpha_i \left[f_j - \frac{\epsilon_j^+}{6}\left(1 - \frac{\alpha_i}{\Delta x}\right)\left(1 + \frac{\alpha_i}{\Delta x}\right)(f_{j+1} - f_j) - \frac{\epsilon_j^-}{6}\left(2 + \frac{\alpha_i}{\Delta x}\right)\left(1 + \frac{\alpha_i}{\Delta x}\right)(f_j - f_{j-1})\right].
\end{aligned}$$

3 Numerical tests

3.1 The linear advection

Let us first consider the problem of linear advection:

$$\frac{\partial f}{\partial t} + v\frac{\partial f}{\partial x} = 0, \quad \forall x \in [-\pi, \pi], \text{ and } f(t, -\pi) = f(t, \pi). \tag{19}$$

Under these assumption and simplification, one can Fourier analyse the schemes using a discrete Fourier transform

$$f_j^n = \sum_{k=0}^{N-1} \hat{f}_k^n \mathrm{e}^{i\,k\,x_j}, \text{ where } \hat{f}_k^n = \sum_{j=0}^{N-1} f_j^n \mathrm{e}^{-i\,k\,x_j}.$$

Then, the solution of (19) in the Fourier space is given by

$$\hat{f}_k^n = \hat{f}_k^0\, \mathrm{e}^{i\,k\,v\,t^n}, \tag{20}$$

In the general situation, the equation (20) is not satisfied by the algorithm, then it is valuable to give the types of numerical error which can occur,

- the amplitude error $\hat{f}_k^n / \hat{f}_k^0$: the harmonic must decay to stabilize the algorithm, which introduces numerical diffusion. These errors are usually most important for short wave length harmonics.
- the phase error $|v\,t^n - Arg(\hat{f}_k^n / \hat{f}_k^0)|$: it is generally called dispersion and describes the error of harmonics which propagate at the wrong speed. The errors are usually increasing with the wave number k.

On the one hand, the amplification factor is plotted (see Fig.1) for the FBM and third order reconstruction without slope corrector (1), and for the semi-lagrangian method with Lagrange (2), Hermite and cubic spline (3) interpolations. Methods using a smooth reconstruction (Hermite or cubic spline) are less dissipative than ones using only a continuous approximation. To obtain a similar amplification factor with the Lagrange interpolation, a polynomial of degree nine is required. The dissipation of the conservative method with a quadratic polynomial is identical to the cubic Lagrange interpolation one. The linear reconstruction used in the (FBM) is the most dissipative. On the other hand, the phase error (see Fig.2) for the semi-lagrangian method using a Hermite reconstruction with fourth order approximation of the derivative is the most important. The cubic spline reconstruction is also less accurate than the Lagrange interpolation of degree nine.

3.2 The Vlasov-Poisson system

In this section, we want to compare different methods and reconstructions for the numerical resolution of the Vlasov-Poisson system with periodic boundary conditions:

$$\frac{\partial f}{\partial t} + \mathrm{div}_x\,(v\,f) + \mathrm{div}_v\,(E(t,x)\,f) = 0 \tag{21}$$

coupled with the normalized Poisson equation

$$E(t,x) = -\nabla_x \phi(t,x), \quad -\Delta\phi(t,x) = \int_{\mathbb{R}^d} f(t,x,v)dv - 1. \tag{22}$$

The time discretization procedure, originally proposed by Cheng and Knorr [5], is based on a splitting algorithm and can be used to go from time step t^n to t^{n+1}

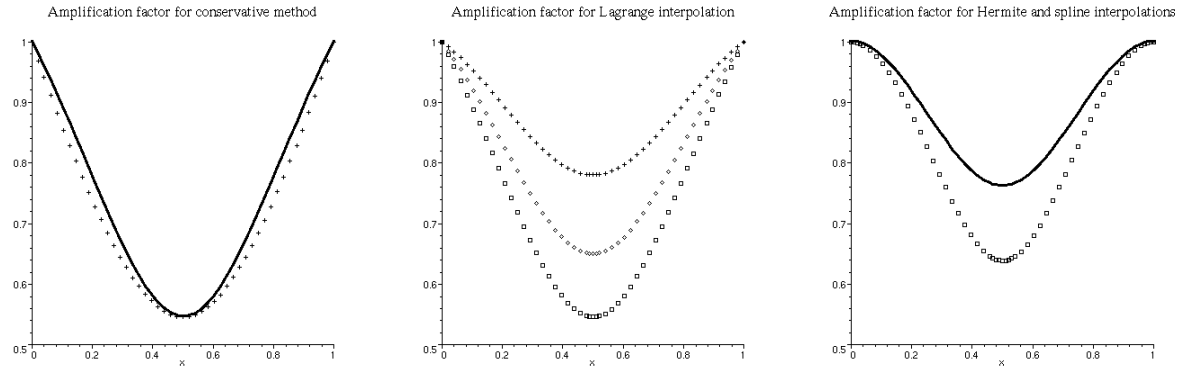

(1) (2) (3)

Figure 1: *The amplification factor with respect to α for a fixed mode k. (1) the classical FBM (cross) and third order reconstruction without slope corrector (line); (2) the semi-lagrangian method with a Lagrange interpolation of degree 3 (box), 5 (diamond), and 9 (cross); (3) and with cubic Hermite polynomial with a fourth order approximation of the derivative (box), and cubic spline interpolation (line).*

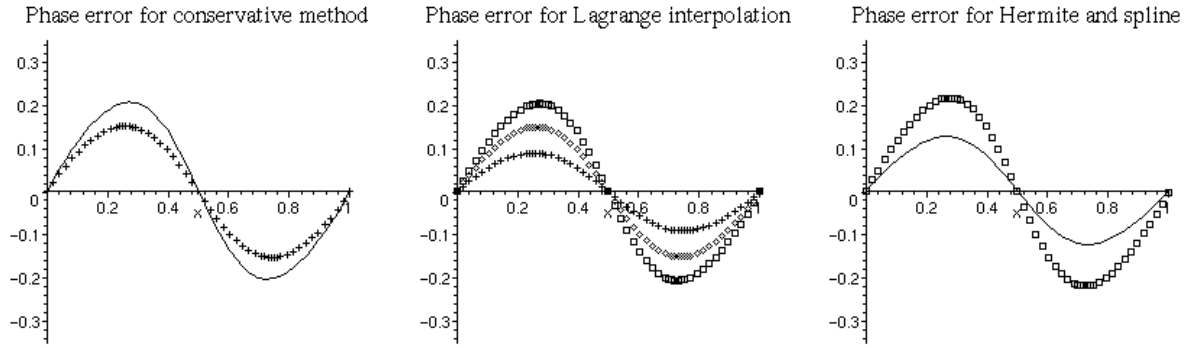

(1) (2) (3)

Figure 2: *The phase error with respect to α for a fixed mode k. (1) the conservative method for the classical FBM (cross) and third order reconstruction without slope corrector (line); (2) the semi-lagrangian method with a Lagrange interpolation of degree 3 (box), 5 (diamond), and 9 (cross); (3) and with cubic Hermite polynomial with a fourth order approximation of the derivative (box), and cubic spline interpolation (line).*

- 1. Perform a half time step shift along the x-axis: $f^*(x,v) = f(t^n, x - v\Delta t/2, v)$.
- 2. Compute the electric field at time $t^{n+1/2}$ by substituting f^* in the Poisson equation.
- 3. Perform a shift along the v-axis: $f^{**} = f^*(x, v - E(t^{n+1/2}, x)\Delta t)$.
- 4. Perform a second half time step shift along the x-axis: $f(t^{n+1}, x, v) = f^{**}(x - v\Delta t/2, v)$.

We now propose classical numerical tests to compare different reconstructions.

A. The linear Landau damping in 1D: The initial data is

$$f(0,x,v) = \frac{1}{\sqrt{2\pi}}\,\mathrm{e}^{-v^2/2}\,(1 + \alpha\cos(k\,x)), \quad \forall (x,v) \in (0,L)\times\mathbb{R},$$

where α=0.01, the periodic length is L=4 π and k=0.5. We are using a number of cells N_x=32 in the x-direction, and N_v=16, 32 and 64 in the v-direction with v_{max}=4.5, and Δt=1/8.

Fig.3 represents the evolution of the electric energy $\sum |E_i(t)|^2$ obtained by the PFC scheme, the fourth order ENO reconstruction and the semi-lagrangian method using a cubic spline interpolation with N_v=32. The recurrence effect appears at T_R=44.68, which is the theoretical time predicted from the free streaming case since $T_R = 2\,\pi/(k\,\Delta v)$. The PFC method first gives a good approximation of the damping rate but when approaching the recurrence time the evolution of the electric field is less accurate, whereas the behavior obtained by the fourth order ENO scheme and the semi-lagrangian method is more stable for long time. In this case, the distribution function obtained with different schemes remains positive, and the relative error norm of variations of the kinetic entropy, L^2-norm, and total energy always stays less than 10^{-5}.

In Fig.4, the basic mode of the electric field k=0.5, obtained by the PFC method, is plotted against time for N_v=16, 32, and 64 cells. It shows the exponential decay of the amplitude of the electric field according to Landau's theory. The damping rate and the frequency of oscillations obtained by this method with only 32 cells in the v direction, are respectively γ=0.153 and ω=1.415, which agree very well with values γ=0.1533 and ω=1.4156 predicted by the theory. The use of a sufficiently large number of cells allows to improve the time evolution of the electric field and gives good results.

B. The strong Landau damping in 1D: In this example, the amplitude of the initial perturbation of the density is increased, we take for the previous initial data α = 0.5 and v_{max}=6. The number of cells is N_x=32 and N_v=64, 128. The previous theory cannot be applied because non linear effects are too important, but this test has been studied by many authors [8, 15, 10]. Results are in good agreement with numerical simulations presented in the literature: the electric energy first decays exponentially and is next periodically oscillating. In Fig.5, the evolution of the electric energy is plotted for the PFC scheme with 32×64 cells, and for the semi-lagrangian method using a cubic spline interpolation with 32×64 and 32× 128 points. The result obtained by the PFC method is much more accurate than one obtained by the semi-lagrangian method using the same grid.

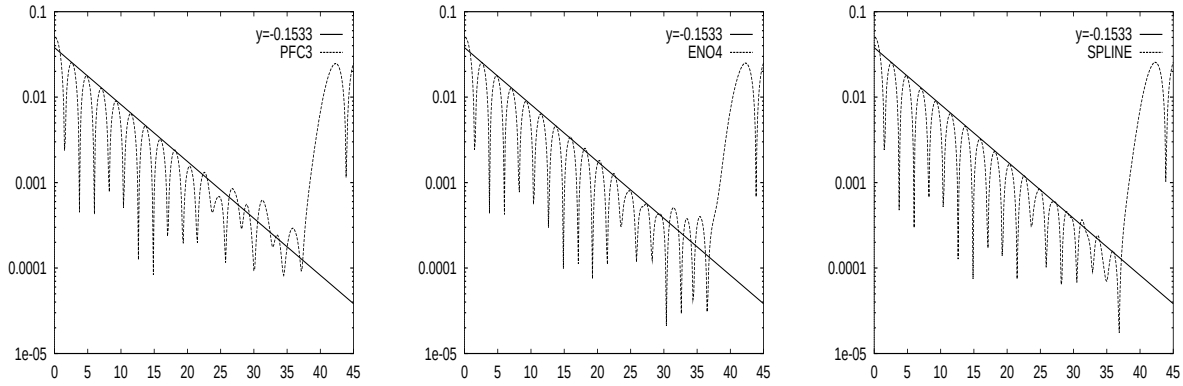

Figure 3: *Time evolution of the electric energy on logarithm scale obtained by the PFC method (1), the fourth order ENO (2), and the cubic spline (3) interpolation with 32×32 unknowns for linear Landau damping.*

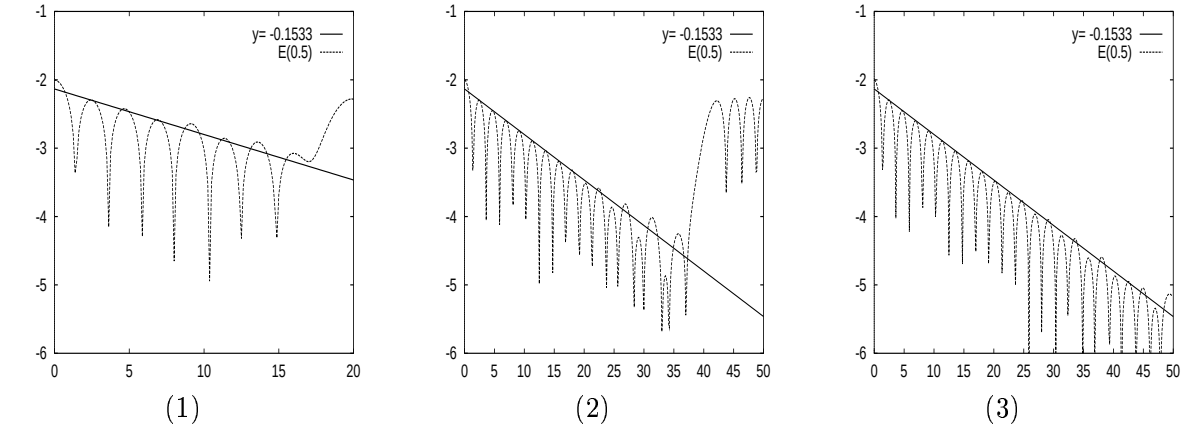

Figure 4: *Time evolution of the first mode of the electric field* $E(t, k = 0.5)$ *obtained by the PFC method with* N_v*=16,* N_v*=32, and* N_v*=64 cells for linear Landau damping*

Next, we are interested by the evolution of the kinetic entropy and L^p-norms which are theoretically conserved. The evolution of the discrete entropy $H(t)=-\sum f_i(t)\ \ln(f_i(t))$, and the discrete $L^p(t)$-norm $\sum |f_i(t)|^p$ for p=1,2 are presented in Fig.6 for the different schemes. The variation of the L^1-norm represents the rate of negative values since the global mass $\sum f_i(t)$ is preserved even for semi-lagrangian methods. On the one hand, the semi-lagrangian method does not preserve positivity and the amplitude of spurious oscillations increases when non linear effects occur. On the other hand, as it is predicted by the Fourier analysis, the conservative method is more dissipative than the semi-lagrangian one since the kinetic entropy strongly decreases. The variation of the stencil of the ENO reconstruction acts as a smoothing effect, then the dissipation is much more important, indeed the kinetic entropy is not well stabilized. The entropy obtained by the PFC scheme is first increasing and is next well stabilized, whereas it is oscillating with the semi-lagrangian method. The strong dissipation of the conservative method can be explained by the averaging step, indeed small details of the distribution function are eliminated to stabilize the scheme. As for the distribution function in the (x, v) space, small bumps appear around the phase velocity $v_\phi = \omega/k$. These bumps represent particles which are trapped by electrostatic waves (see Fig.7). As a consequence of the entropy decay, the distribution function is smoothed when filaments become smaller than the phase space grid size. Nevertheless, this smooth approximation seems to give a good description of macroscopic values (physics quantities obtained by the integration of moments of the distribution function with respect to v) since the evolution of the electric energy is more accurate than one obtained from the semi-lagrangian method using the cubic spline interpolation. Moreover, the variation of the total energy is less than 2% for all schemes excepted for the ENO method for which the variation of the total energy is increasing and the amplitude of the electric energy is damped. Then, the ENO reconstruction does not seem to be well adapted to treat non linear effects.

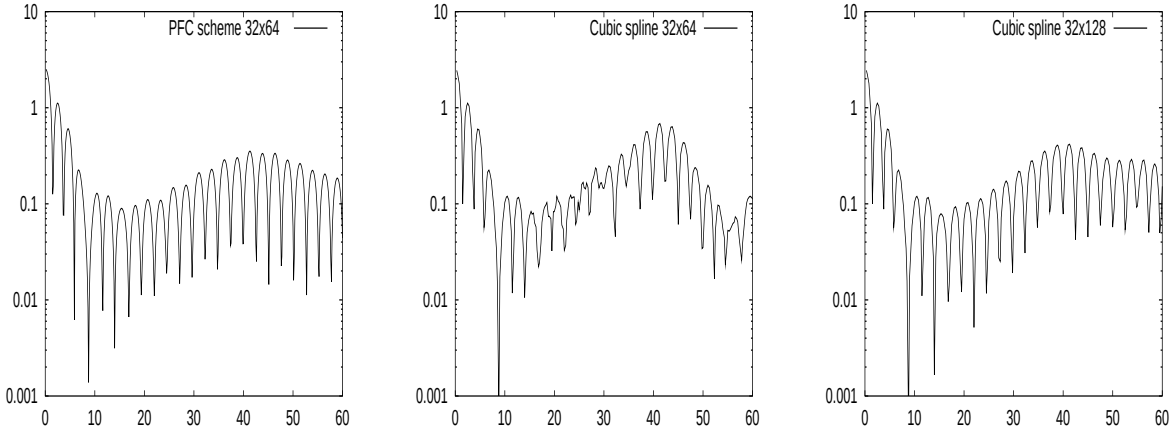

(1) (2) (3)

Figure 5: *Time evolution of the discrete electric energy in logarithm scale for the PFC scheme 32×64 (1); the cubic spline interpolation with 32×64 (2) and 32×128 (3) unknowns for strong Landau damping.*

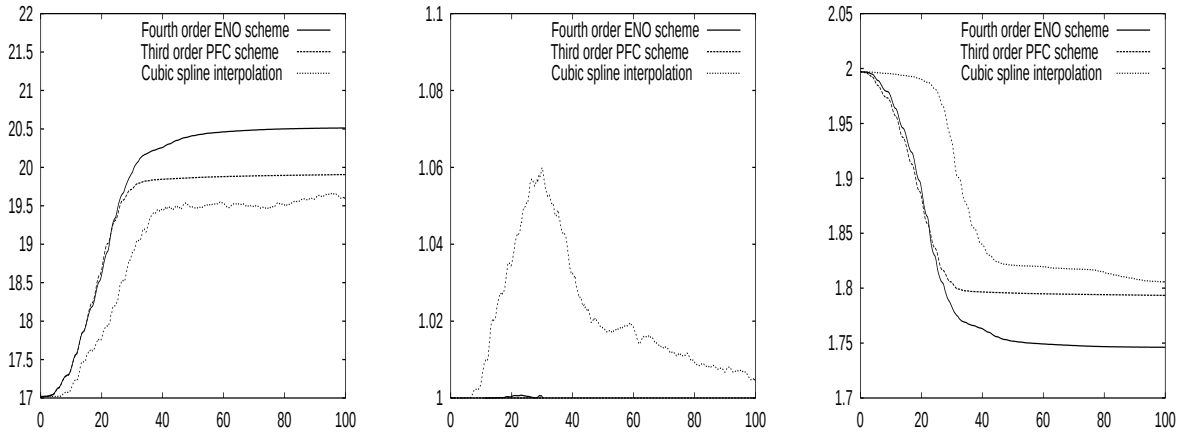

Figure 6: *Time evolution of the discrete kinetic entropy, L^1 and L^2 norms with 32×64 unknowns for strong Landau damping.*

C. The linear Landau damping in 2D: The initial condition is set to

$$f_0(x,y,v_x,v_y) = \frac{1}{2\pi}\mathrm{e}^{-(v_x^2+v_y^2)/2}\,(1\,+\,\alpha\cos(k_x\,x)\cos(k_y\,y)),$$

with $\alpha = 0.05$, the velocity space is truncated at v_{max}=6, the wave numbers are k_x=k_y=0.5, and the length of the periodic box in the physical space is L_x=L_y=$4\,\pi$. Finally, the four dimensional grid contains 64 points per direction and the time step is set to Δt=1/8. From the symmetry of the initial data, the evolution of two components of the electric field are identical. In Fig. 9, we report the evolution of the electric energy obtained by the PFC scheme and the semi-lagrangian method using a cubic spline interpolation. The two methods give an accurate damping of the amplitude of the electric field. The Fourier modes of the electric field obtained by the PFC scheme are plotted in Fig. 10. It shows the exponential decay of the modes $E_x(t, k_x = 0, k_y = 0.5)$ and $E_x(t, k_x = 0.5, k_y = 0.5)$ with a damping rate respectively γ = -0.1533 and γ=-0.394, and the frequency of oscillations ω=1.4156 and ω=1.6973, which are the theoretical values predicted by the linear Landau theory.

D. The evolution of a beam in 2D: We now consider the evolution of a RMS matched semi-Gaussian beam in a uniform focusing channel in the four dimensional phase space. In this case the Vlasov equation has the following form, for all $\mathbf{x} = (x, y)$, and $\mathbf{v} = (v_x, v_y)$,

$$\frac{\partial f}{\partial t}\,+\,\mathbf{v}.\nabla_{\mathbf{x}} f\,+\,(E_{self}(t,\mathbf{x}) + E_{appl}(t,\mathbf{x})).\nabla_{\mathbf{v}}\,f\,=\,0, \tag{23}$$

where E_{self} is the self-consistent electric field given by the Poisson equation and E_{appl} is a linear external electric field allowing to focalize the beam. The initial value of the distribution function is

$$f_0(x,y,v_x,v_y) = \frac{n_0}{(2\,\pi\,v_{th}^2)\,(\pi\,a^2)}\mathrm{e}^{-\frac{v_x^2+v_y^2}{2\,v_{th}^2}}, \quad \text{if } x^2+y^2 \le a^2,$$

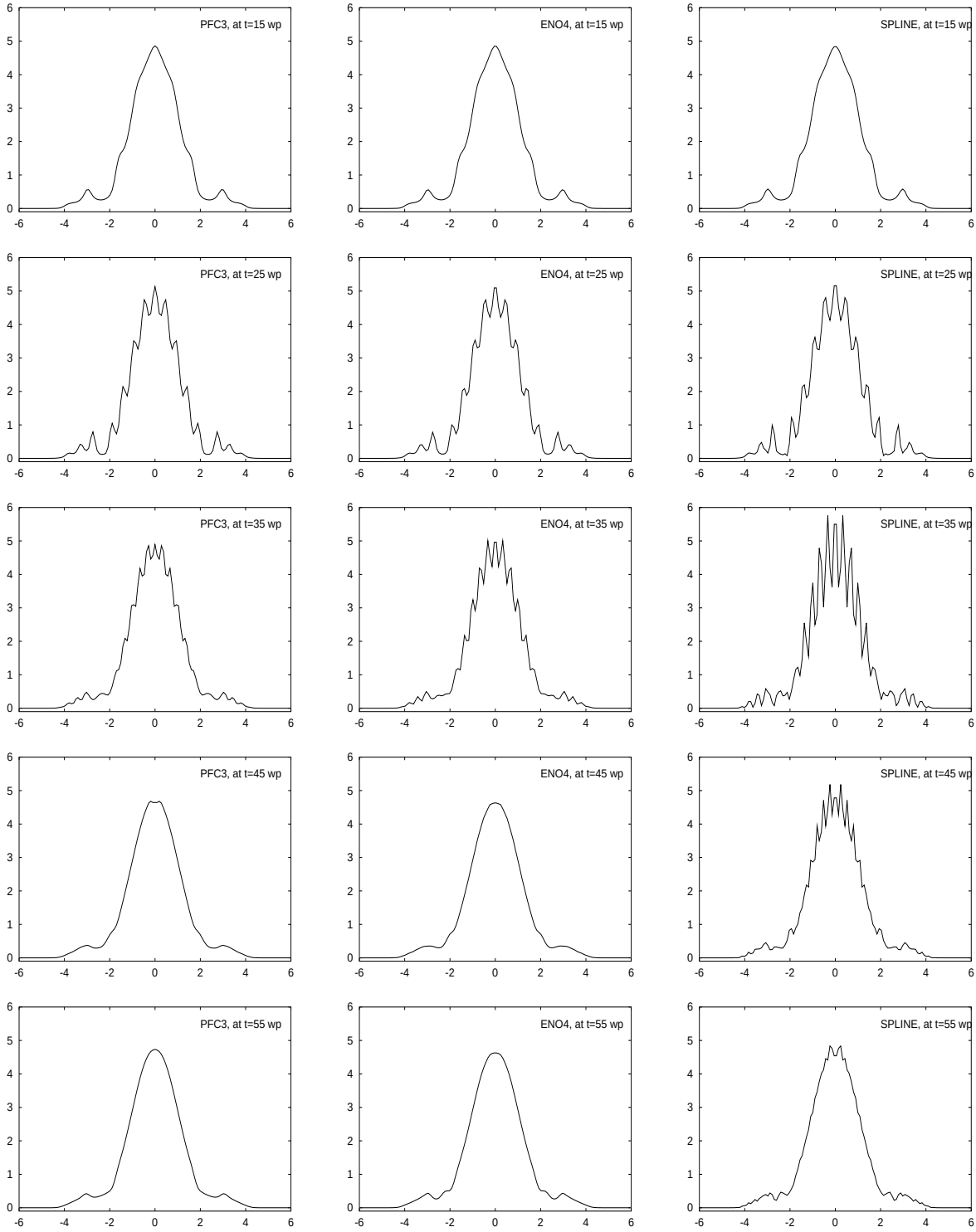

Figure 7: *Time development of the spatially integrated distribution function for the PFC scheme (left); the fourth order ENO reconstruction (centre) and the cubic spline (right) interpolation for strong Landau damping.*

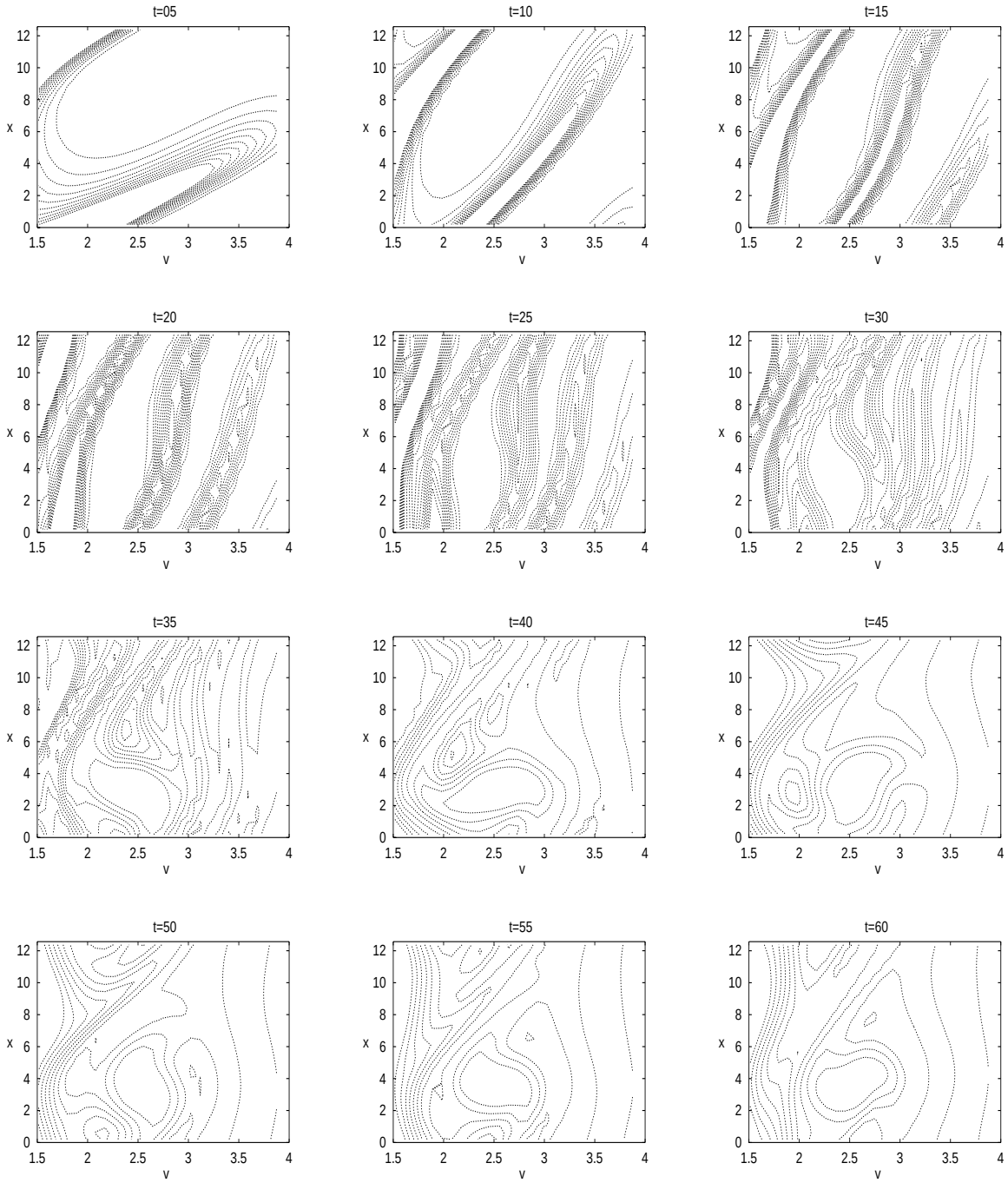

Figure 8: *Time development distribution function* $f(t,x,v) \leq 0.1$ *obtained by the PFC scheme for strong Landau damping.*

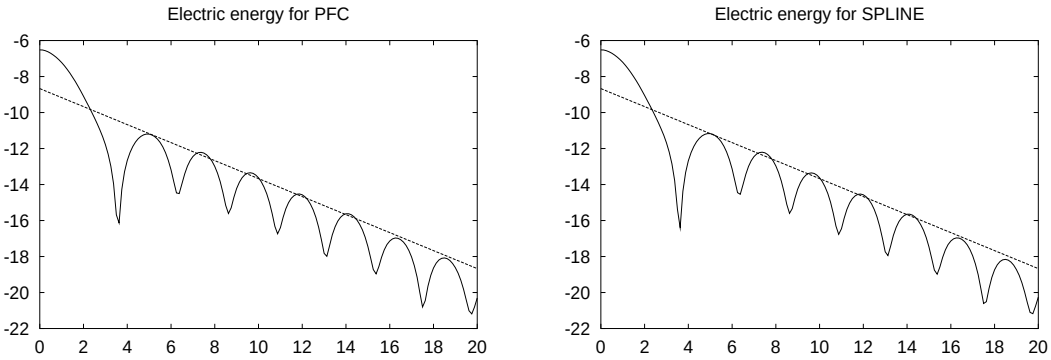

Figure 9: *Time evolution of the electric energy* $(\Delta x \sum_i E_i^2)^{1/2}$ *on logarithm scale obtained by the PFC and SPLINE methods with 64×64 unknowns for the 2D linear Landau damping.*

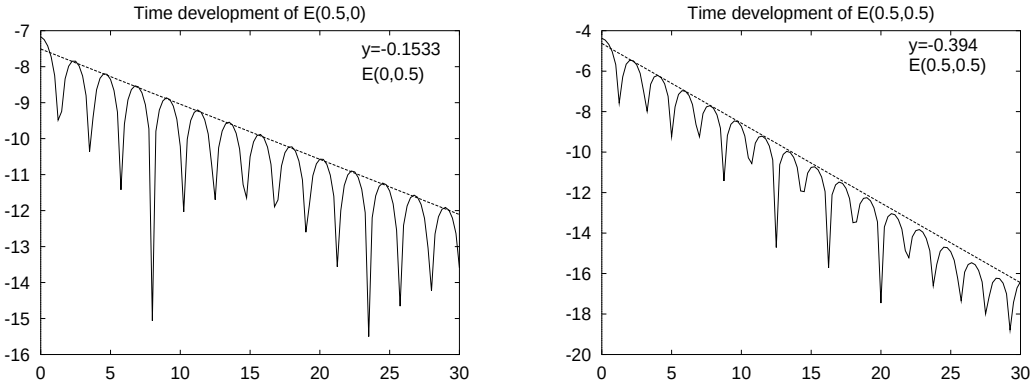

Figure 10: *Time evolution of the basic modes* $E_x(0.5, 0)$ *and* $E_x(0.5, 0, 5)$ *on logarithm scale obtained by the PFC method with 64×64 unknowns for the 2D linear Landau damping.*

and $f_0(x, y, v_x, v_y) = 0$, if $x^2 + y^2 > a^2$. The RMS thermal velocity v_{th} is computed such that the beam is matched (see [11]): we consider the KV-distribution function which is a stationary solution of the Vlasov equation (23) and the self consistent electric field is linear with respect to the x variable, then

$$E_{self}(t, \mathbf{x}) + E_{appl}(t, \mathbf{x}) = -\omega^2 \, \mathbf{x}.$$

and the initial data is

$$f_0(\mathbf{x}, \mathbf{v}) = \delta_{\mathcal{C}}, \quad \text{with } \mathcal{C} = \{\frac{x^2}{A^2} + \frac{y^2}{A^2} + \frac{v_x^2}{(\omega\, A)^2} + \frac{v_y^2}{(\omega\, A)^2} = 1\}.$$

Then, the RMS values are given by

$$\sqrt{\overline{x^2}} = \sqrt{\frac{\int x^2 \, f d\mathbf{x}\, d\mathbf{v}}{\int f d\mathbf{x}\, d\mathbf{v}}} = A, \quad \sqrt{\overline{v_x^2}} = \sqrt{\frac{\int v_x^2 \, f \, d\mathbf{x}\, d\mathbf{v}}{\int f d\mathbf{x}\, d\mathbf{v}}} = \omega\, A,$$
$$\sqrt{\overline{y^2}} = \sqrt{\frac{\int y^2 \, f d\mathbf{x}\, d\mathbf{v}}{\int f d\mathbf{x}\, d\mathbf{v}}} = A, \quad \sqrt{\overline{v_y^2}} = \sqrt{\frac{\int v_y^2 \, f \, d\mathbf{x}\, d\mathbf{v}}{\int f d\mathbf{x}\, d\mathbf{v}}} = \omega\, A,$$

Now, for the semi-Gaussian beam, the initial self-consistent electric field can be easily computed since it is also linear in $\mathbf{x}$. Then, we take

$$\overline{x^2} = \overline{y^2} = a^2/4, \quad v_{th}^2 = \overline{v_x^2} = \overline{v_y^2} = \omega^2 a^2/4.$$

and ω^2 represents the difference between the initial self consistent electric field and the linear applied field $E_{appl}(t, x)$=-$\omega_0^2\, x$. In this example, we have chosen ω and ω_0 such that the tune depression $\frac{\omega}{\omega_0}$=1/2. The beam density n_0 can be written with respect to the current I and the beam velocity v_b, by $n_0 = \frac{I}{q\, v_b}$. The beam is assumed to be composed of ionized particles of potassium, the current I=0.2 A, the beam velocity v_b=0.63 $\times 10^6$ m/s and the radius of the beam is a=0.02 m. We compare the evolution of the beam obtained by the PFC algorithm using the third order positive reconstruction with the semi-lagrangian method using the cubic spline interpolation (see [14]).

In table 1, we present the total time computation for the semi-lagrangian method and the PFC scheme. It is evident that the PFC scheme is faster than the semi-lagrangian method since the reconstruction is local. Contour plots of the phase space projections as well as slices of the charge density and the electric field obtained by the PFC method are given in the following figures. We notice that the beam at first becomes hollow, then regions of high density propagate to the core of the beam and out again, creating space charge waves. These waves are damped by phase mixing after a few lattice periods. Results obtained by the PFC method seem to be very close to those obtained by the semi-lagrangian method.

4 Conclusion

In this paper, we introduced a new method to solve the Vlasov equation using a phase space grid. This method enforces the conservation of the global mass (or the number of particles) and

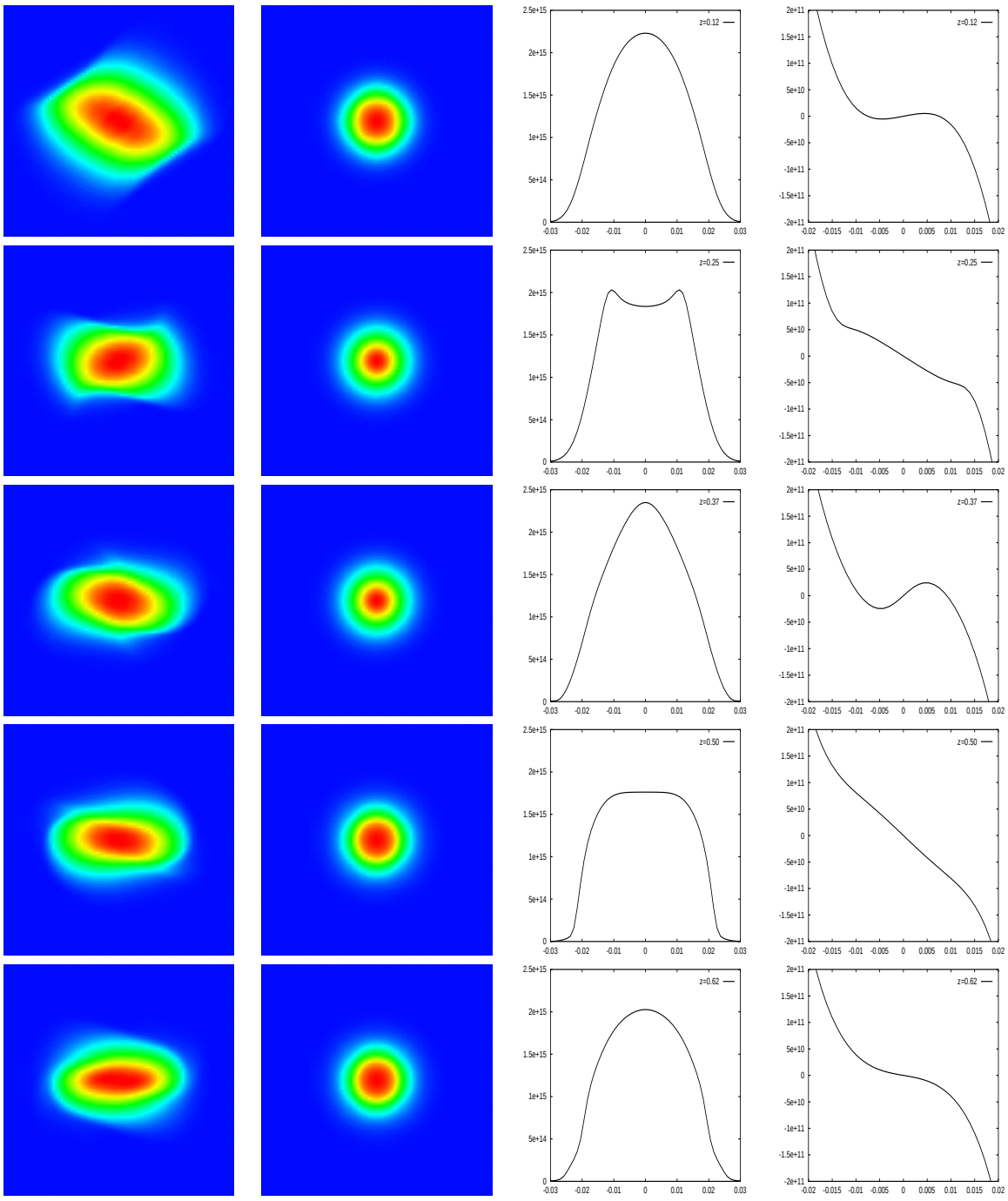

Figure 11: *Time development of (1) x-v_x projection, (2) v_x-v_y projection, (3) slice of charge density (4) slice of the total electric field obtained by the PFC method.*

Number of processors	PFC scheme	SPLINE method
2 processors	4 h 30 min	6 h 20 min
4 processors	2 h 11 min	3 h 07 min
8 processors	56 min	84 min

Table 1: *Total computation time for PFC3 and SPLINE methods with respect to the number of processors for a grid size* $64 \times 64 \times 64 \times 64$ *points.*

controls numerical oscillations using the stencil variation technique (ENO reconstruction) or the preservation of positivity (PFC). Moreover, it allows to treat strong non linear problems without numerical instabilities. On the one hand, numerical results show the ENO approximation is too dissipative to describe accurately the distribution function, because the entropy and the L^2 norm are strongly decreasing. On the other hand, the PFC scheme is almost as accurate as the semi-lagrangian method using a cubic spline interpolation, and the preservation of positivity allows to have a better long time description of macroscopic values like the charge density, or the electric field. Moreover, the local reconstruction is well suited to do parallel computation in high dimension.

Actually, this method seems to be a good alternative to the PIC methods to deal with strongly non linear problems in two or four dimensional phase space.

References

[1] C. K. Birdsall, A. B. Langdon *Plasma Physics via Computer Simulation Institute of Physics Publishing, Bristol and Philadelphia.*, (1991)

[2] F. Bouchut, F. Golse, M. Pulvirenti, *Kinetic equations and asymptotic theory Gauthier-Villars, series in Applied Mathematics*, (2000)

[3] J. P. Boris, D. L. Book, Flux-corrected transport. I: SHASTA, a fluid transport algorithm that works. *J. Comput. Phys.*, 11: (1973) pp. 38–69.

[4] J. P. Boris, D. L. Book, Flux-corrected transport. III: Minimal-error FCT algorithms. *J. Comput. Phys.*, 20: (1976) pp. 397–431.

[5] Cheng, G. Knorr, The integration of the Vlasov equation in configuration space. *J. Comput. Phys.*, 22: (1976) pp. 330–348.

[6] E. Fijalkow, A numerical solution to the Vlasov equation. *Comput. Phys. Communications*, 116: (1999) pp. 319–328.

[7] A. Harten, S. Osher, Uniformly High-Order Accurate Non-Oscillatory Schemes. I. *SIAM Numer. Anal.*, 24: (1987) pp. 279–309.

[8] A. J. Klimas, A method for overcoming the velocity space filamentation problem in collisionless plasma model solutions. *J. Comput. Phys.*, 68: (1987) pp. 202–226.

[9] A. Klimas, W. M. Farrell A Splitting Algorithm for Vlasov Simulation with Filamentation Filtration. *J. Comput. Phys.*, 110: (1994) pp. 150–163.

[10] G. Manfredi, Long time behavior of non linear Landau damping. *Phys. Rev. Letters.*, 79 -15: (1997) pp. 2815–2818.

[11] M. Reiser, Theory and design of charged particle beams *Wiley and sons*, (1994).

[12] M. Shoucri, G. Knorr, Numerical integration of the Vlasov equation. *J. Comput. Phys.*, 14 -1: (1974) pp. 84–92.

[13] E. Sonnendrücker, J. Roche, P. Bertrand, A. Ghizzo, The Semi-Lagrangian Method for the Numerical Resolution of Vlasov Equations. *J. Comput. Phys.* , 149: (1999) pp.201–220.

[14] E. Sonnendrücker, J.J. Barnard, A. Friedman, D.P. Grote, S.M. Lund, Simulation of heavy ion beams with a semi-Lagrangian Vlasov solver Proceedings of the HIF 2000 symposium.

[15] T. Nakamura, T. Yabe, Cubic interpolated propagation scheme for solving the hyper-dimensional Vlasov-Poisson equation in phase space. *Comput. Phys. Communications*, 120: (1999) pp. 122–154.

[16] S. I. Zaki, L. R. Gardner, T. J. M. Boyd, A finite element code for the simulation of one-dimensional Vlasov plasmas I. Theory *J. Comput. Phys.*, 79: (1988) pp. 184–199.

[17] S. I. Zaki, L. R. Gardner, T. J. M. Boyd, A finite element code for the simulation of one-dimensional Vlasov plasmas II. Applications *J. Comput. Phys.*, 79: (1988) pp. 200–208.